

# Robust $H_\infty$ Design of an Automotive Cruise Control System

Balázs Németh\* Péter Gáspár\* Rodolfo Orjuela\*\*  
Michel Basset\*\*

\* *Systems and Control Laboratory, Institute for Computer Science and Control, Hungarian Academy of Sciences, Kende u. 13-17, H-1111 Budapest, Hungary*

*E-mail: [balazs.nemeth,peter.gaspar]@sztaki.mta.hu*

\*\* *Modelling Intelligence Process and Systems (MIPS) Laboratory EA2332 Université de Haute-Alsace, 12 rue des frères Lumière, F-68093 Mulhouse Cedex, France*

*E-mail: [rodolfo.orjuela, michel.basset]@uha.fr*

---

**Abstract:** Advanced Driver Assistance Systems (ADAS) are in the focus of the vehicle control research. In the paper, the design method of a controller for a longitudinal ADAS system of a test vehicle is proposed. The cruise control must guarantee precise velocity tracking at varying vehicle mass and road inclinations. The mass variation and road slope changes are formulated as disturbances of the system. A combined robust  $\mathcal{H}_\infty$  and feedforward control design method is applied, which guarantees the robustness of the system against disturbances and considers actuator dynamics. The resulting control algorithm is implemented in CarSim. Simulation scenarios on the Mulhouse-Belfort highway section are performed to illustrate the efficiency of the method.

*Keywords:* Advanced Driver Assistance Systems, cruise control, robustness, optimal control

---

## 1. INTRODUCTION AND MOTIVATION

In the last few decades, Advanced Driver Assistance Systems (ADAS) have been developed to improve the safety and efficiency of road vehicles. The active control systems are able to assist or give warning signals to the driver in e.g. trajectory tracking, parking or critical situations. The designed ADAS systems must guarantee several performances and robustness in various vehicle dynamic maneuvers. The motivation of the paper is to develop a cruise control algorithm which is incorporated in an ADAS system on the test vehicle of the Modelling Intelligence Process and Systems (MIPS) Laboratory, see Figure 1. The vehicle is used for the validation of the developed ADAS concept. An applicative requirement for the control system is the adaptivity to the current circumstances of the vehicle. Therefore, the control system must be robust and it is necessary to use only a small number of vehicle parameters.

Several methods in the topic of cruise control systems have been proposed. Model Predictive Control (MPC) algorithm is largely employed for cruise control purposes. Borrelli et al. (2001) proposes a hybrid discrete vehicle model with piecewise affine functions, where the frictional torque is approximated as a piecewise affine function of the slip. Moreover, constraints on the torque, on its varia-



Fig. 1. Test vehicle

tion, and on the slip are satisfied. The MPC technique is applied to consider the constraints and solve the traction control problem and the robustness is proved based on experimental results. A two-level control design is proposed in Li et al. (2011). In the architecture the low level controller handles the nonlinearities in the vehicle dynamics (engine torque maps, time-varying gear position and aerodynamic drag force), while the high level is an MPC control, considering minimal tracking error, fuel consumption and the car-following requirements of the driver. Safety and comfort criteria are involved as constraints during a quadratic programming algorithm. In Katriniok et al. (2013) a velocity tracking problem as part of an integrated lateral and longitudinal control is proposed. In the vehicle model the longitudinal acceleration is handled as control input, whose constraints are incorporated in the MPC formulation.

The sliding-mode control technique is used in Lu and Hedrick (2005). In the paper, a second-order nonlinear vehicle body dynamical model is adopted, which is feed-

---

\* Acknowledgment: The research and the paper has been supported by CampusFrance and the János Bolyai Research Scholarship of the Hungarian Academy of Sciences

back linearizable. Besides the vehicle dynamics, other main dynamical components along the power-train and drive-train are also modeled, such as a turbocharged diesel engines, torque converters, transmissions, transmission retarders, pneumatic brakes and tyres. A two-level control design is proposed, where the purpose of the sliding-mode high level control is to generate the desired torque from the desired vehicle acceleration. Robustness in the control architecture against the external disturbances is considered. Kolmanovsky and Filev (2010) focus on the longitudinal control in such a way as to achieve optimal trade-off between expected average fuel economy and expected average travel speed. An optimal control problem is formulated using Bellman's principle. The optimal control policy is computed offline, while the vehicle speed set-point (one distance step ahead) is computed on-line. Recently, in Attia et al. (2014) a longitudinal control strategy based on a two-loop approach has been presented. The direct Lyapunov approach is considered to design the outer-loop for references speed tracking and the inner-loop for torque control. This longitudinal control is coupled to a lateral control providing a whole guidance control strategy.

Considering PI structured adaptive control design, an approach is presented by Xu and Ioannu (1994). The design is based on a linearized vehicle model, while a reference model generates the reference velocity signal. The adaptation guarantees the handling of model parameter variations. A model-free control design approach is applied to design an intelligent PI controller in Menhour et al. (2013). The longitudinal control inputs are traction/braking wheel torques, and the longitudinal positioning error of the vehicle is improved using the method. The method is robust with respect to modeling errors and parametric uncertainties. A combined  $\mathcal{H}_\infty$  feedback and feedforward control is employed to damp out longitudinal oscillations using  $\mu$  analysis in Lefebvre et al. (2003). The robust  $\mathcal{H}_\infty$  method is compared to the Linear Quadratic Regulator design in Junaid et al. (2005). In the paper a third-order linear system is applied, which describes the dynamics of the vehicle and the power-train. The controlled system is robust against exogenous disturbances and the parameter uncertainty of power-train time is constant.

The goal of this paper is to design a velocity tracking longitudinal vehicle control which guarantees robust performance. The contribution of the paper is a robust  $\mathcal{H}_\infty$  cruise control based on a feedforward and a feedback control design, which guarantees a precise velocity tracking against longitudinal disturbance effects, such as road slopes, aerodynamic forces, rolling resistance, and mass parameter variations of the vehicle. In the control formulation the dynamics (parameter variation) of the actuator has been considered in a simplified form.

The paper is organized as follows. Section 2 describes the formulation of the longitudinal vehicle model together with the mass variation and disturbances. The robust optimal control strategy is proposed in Section 3. The efficiency of the method is illustrated through simulation examples in Section 4. Finally, the last section summarizes the contributions of the paper and the further works.

## 2. MODELING LONGITUDINAL DYNAMICS

In this section the modeling of longitudinal dynamics is presented. Since the cruise control method must be easily adopted to a vehicle, some vehicle parameters are involved. Thus, the longitudinal dynamics is described in the approach by the next simplified model:

$$m\dot{v} = F_l - F_d \quad (1)$$

where  $m$  is the mass of the vehicle,  $v$  is the longitudinal velocity,  $F_l$  is the realized longitudinal force on the wheels.  $F_d$  includes the longitudinal disturbances, such as the aerodynamic forces, rolling resistance and road slope.  $F_d$  is expressed as:

$$F_d = C_a v^2 + C_r g m \cos \vartheta + m g \sin \vartheta \quad (2)$$

where  $\vartheta$  is road slope and  $C_a$ ,  $C_r$  are vehicle parameters related to aerodynamic and resistances forces.

Since the handling of vehicle mass uncertainty is a requirement for the control system, it is considered defining the actual mass  $m$  of the vehicle such as:

$$m = m_0 + m_v \quad (3)$$

where  $m_0$  is the nominal mass of the vehicle and  $m_v$  is the mass variation. The variation is assumed to be a bounded parameter, e.g.  $m_v/m_0 = \pm 30\%$ . Substituting (3) in (1), the longitudinal motion equation is reformulated in the following way:

$$(m_0 + m_v)\dot{v} = F_l - F_d \quad (4a)$$

$$m_0\dot{v} = F_l - F_d - m_v\dot{v} \quad (4b)$$

Considering that  $\dot{v}$  actual longitudinal acceleration is a measurable and (practically) bounded signal of the vehicle,  $m_v\dot{v}$  is handled as a disturbance of the vehicle. Combining it with  $F_d$ , the next expression is yielded:

$$\begin{aligned} F_d + m_v\dot{v} &= C_a v^2 + C_r g (m_0 + m_v) \cos \vartheta \\ &\quad + (m_0 + m_v) g \sin \vartheta + m_v \dot{v} \\ &= (C_a v^2 + C_r g m_0 \cos \vartheta + m_0 g \sin \vartheta) \\ &\quad + m_v (C_r g \cos \vartheta + g \sin \vartheta + \dot{v}) \\ &= F_{d,1} + m_v f_{d,2} \end{aligned} \quad (5)$$

Note that expression (5) contains two different elements.  $F_{d,1}$  and  $f_{d,2}$  incorporate measurable signals, such as velocity, road slope and longitudinal acceleration. Thus,  $F_{d,1}$  is handled in this approach as a measured disturbance. Since there is no information about the mass variation  $m_v$ , the term  $m_v f_{d,2}$  is considered as an unknown disturbance - where actually  $f_{d,2}$  is a measurable part of the disturbance expression.

## 3. ROBUST CONTROL STRATEGY

In this section the control design for the longitudinal velocity tracking control problem is proposed. The controlled system must guarantee precise tracking, robustness against the mass variation, road slope and further disturbances. The conservativeness of the control algorithm can be reduced through the consideration of the measurements on disturbances. In the proposed control scheme,  $F_{d,1}$  is considered as a measured disturbance. Thus, it is recommended to derive a feedforward term in the control strategy for the direct elimination of  $F_d$ . In the following a robust control design method is presented, which combines

the advantages of the feedforward and feedback control design.

The realized total longitudinal control force on the wheels  $F_l$  is divided into two elements:

$$F_l = F_{l,0} + F_{l,1} \quad (6)$$

where the purpose of  $F_{l,1}$  is to compensate for the measured disturbance  $F_{d,1}$ , while  $F_{l,0}$  guarantees the unknown disturbance rejection and the performances.

If  $F_{d,1}$  is fully compensated for, then the feedforward control input is

$$F_{l,1} = F_{d,1} = C_a v^2 + C_r g m_0 \cos \vartheta + m_0 g \sin \vartheta \quad (7)$$

where  $v, \vartheta$  are measured and estimated parameters, see Vahidi et al. (2005). Thus, the efficiency of the feedforward disturbance compensation is based on the accuracy of  $v, \vartheta$ . Since the measurement of the speed and the estimation of the road slope are inaccurate, the feedforward compensation has an error  $F_{d,11}$ . The longitudinal motion of the vehicle is formed using (1), (6) and (7) and is described as

$$m_0 \dot{v} = F_{l,0} + F_{l,1} - F_{d,1} - F_{d,11} - f_{d,2} m_v \quad (8a)$$

$$= F_{l,0} - F_{d,11} - f_{d,2} m_v \quad (8b)$$

In the next step a feedback control input  $F_{l,0}$  is designed, which is able to handle the disturbances  $F_{d,11}, f_{d,2} m_v$  in (8a).

### Modeling actuator dynamics

In the real intervention of the driveline/brake system the physical construction of the actuator has an important role. Generally, the actuators delay the intervention and provide additional dynamic motion. Therefore, it is necessary to consider the dynamics of the actuator in the design of the controller to improve the tracking capability of the ADAS system. In the following a simplified formulation of the actuator dynamics, which generates the longitudinal force  $F_l$ , is considered as:

$$\dot{F}_l = -\frac{1}{\tau} F_l + \frac{1}{\tau} u \quad (9)$$

where  $u$  is the control input, which is computed by the control algorithm. The robust control design is based on the relation (9) between  $u_0$  and  $F_{l,0}$ . The considered actuator dynamics (9) for the feedback design can be reformulated as a transfer function:

$$G(s) = \frac{1}{\tau s + 1} = 1 - \frac{\tau s}{\tau s + 1} \quad (10)$$

The reformulation of the actuator dynamics can be handled as an input multiplicative uncertainty of the system, where  $W_u = -\tau s / (\tau s + 1)$  is the uncertainty of the system. In this case, the robustness of the system requires the consideration of the highest bound of  $W_u$  in the control design. The Bode amplitude diagram of  $W_u$  depends on  $\tau$ . Since the maximum bound  $W_u$  is defined by the highest  $\tau$  value, the robust control must be designed with it. The maximum  $\tau$  is related to the slowest actuation of the driveline/braking systems. This  $\tau$  value must be considered in the robust control design.

### Design of feedback controller

The feedback control input  $F_{l,0}$  has three main goals in the control strategy: the rejection of unknown disturbances

$(F_{d,11}, f_{d,2} m_v)$ , the handling of the unmodelled actuator dynamics, and the guaranteeing of the performances. The state-space representation of the system is the following:

$$[\dot{v}] = [0] [v] + \begin{bmatrix} -\frac{1}{m_0} & -\frac{1}{m_0} \end{bmatrix} \begin{bmatrix} F_{d,11} \\ F_{d,2} \end{bmatrix} + \left[ \frac{1}{m_0} \right] F_{l,0} \quad (11a)$$

where the disturbances are compressed to a vector  $F_{d,fb} = [F_{d,11} \ F_{d,2}]^T$ , where  $F_{d,2} = f_{d,2} m_v$ . The measured output of the system is the velocity  $v$ , which is also the state in the formulation.

The performances of the system are the tracking of the reference velocity  $v_{ref}$  and the minimization of the control input  $u_0$ . Note that the influence on control input is necessary to avoid the extremely high actuation of the longitudinal control. The performance signals are

$$|z_1| = |v_{ref} - v| \rightarrow \min \quad (12a)$$

$$|z_2| = |u_0| \rightarrow \min \quad (12b)$$

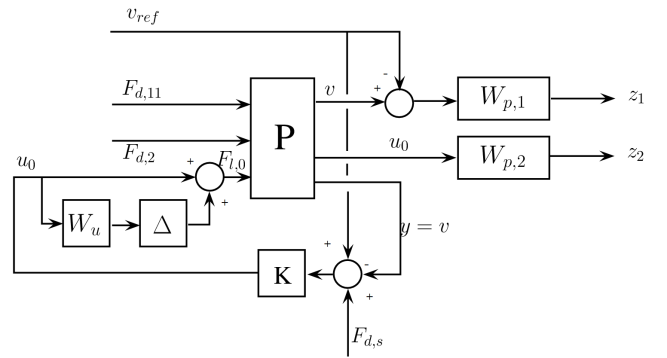


Fig. 2. Closed-loop interconnection

The state-space representation of the system for the control design, which incorporates the performances and the measurement is the following:

$$\dot{x} = Ax + B_1 F_{d,fb} + B_2 u_0 \quad (13a)$$

$$z = C_1 x + D_{1,2} u_0 \quad (13b)$$

$$y = C_2 x \quad (13c)$$

The augmented-plant for the  $\mathcal{H}_\infty$  design is illustrated in Figure 2. The weighting functions of  $z_1$  and  $z_2$  are formulated as  $W_{p,i} = (b_{1,i}s + b_{0,i}) / (a_{1,i}s + a_{0,i})$  where  $b_{1,i}, b_{0,i}, a_{1,i}, a_{0,i}$  are design parameters. The selection of these parameters has significant relevance. The accuracy of the velocity tracking, the limitation of the actuator intervention and the overshoot of the velocity signal are determined by these parameters. In Figure 2 the measured signal is  $y = v$ . The sensor noise  $F_{d,s}$  on the velocity measurement is considered as a disturbance, which must be rejected by the robust controller. Thus,  $F_{d,fb}$  is extended with the signal  $F_{d,s}$ .

The state space representation of the closed-loop control system is formulated in the following way:

$$\dot{x}_{cl} = A_{cl} x_{cl} + B_{cl} w \quad (14a)$$

$$z = C_{cl} x_{cl} + D_{cl} w \quad (14b)$$

The objective of  $\mathcal{H}_\infty$  control is to minimize the inf-norm of the transfer function  $T_{z_\infty w}$ . More precisely, the problem can be stated as follows (Scherer and Weiland, 2000; Boyd et al., 1997). The LMI problem of  $\mathcal{H}_\infty$  performance is formulated as: the closed-loop RMS gain from  $w$  to  $z_\infty$

does not exceed  $\gamma$  if and only if there exists a symmetric and definite positive matrix  $X_\infty$  such that

$$\begin{bmatrix} A_{cl}X_\infty + X_\infty A_{cl}^T & X_\infty B_{cl} & C_{cl}^T \\ B_{cl}^T X_\infty & -\gamma I & D_{cl}^T \\ C_{cl} & D_{cl} & -\gamma I \end{bmatrix} < 0 \quad (15)$$

with  $\gamma > 0$ .

For the open-loop plant  $P$ , see Figure 2, find an admissible control  $K$  which satisfies the following design criteria:

- the closed-loop system must be asymptotically stable,
- the closed-loop transfer function from  $F_{d,fb}$  to  $z_\infty$  satisfies the constraint:

$$\|T_{z_\infty F_{d,fb}}(s)\|_\infty < \gamma, \quad (16)$$

for a given real positive value  $\gamma$ ,

where  $T_{z_\infty F_{d,fb}}(s)$  is cosensitivity function.

Finally, a robust dynamic  $K$  controller is yielded. The feedback control input is formally computed as  $u_0 = K(v_{ref} - v)$ . As a result of the combined feedforward-feedback strategy, the control law of the system, using (7), is yielded as:

$$u = K(v_{ref} - v) + C_a v^2 + C_r m_0 \cos \vartheta + m_0 g \sin \vartheta \quad (17a)$$

$$u = u_0 + u_1 \quad (17b)$$

where  $u_0$  represents the feedback control input and  $u_1$  the feedforward control.

#### Application of the method in the driving/braking system

The result of the robust control design is the longitudinal force input  $u = F_l$ . However, the real physical system has two inputs, such as driveline and brake inputs. The transformation of  $F_l$ , considering the real physical inputs, is presented in the following.

In the conventional engine-powered driveline system the gear positioning and the throttle are the intervention possibilities. The proposed method considers an automatic transmission, where the positioning of the gear is determined by the engine speed and the throttle  $\alpha \in [0 \dots 1]$ . Thus, it is necessary to find an appropriate  $\alpha$ , which guarantees the realization of  $F_l$ . Since the driveline dynamics (9) is faster than the longitudinal dynamics, the transients of the driveline are ignored in the computations. The conversion between  $F_l$  and  $\alpha$  is based on static relations.

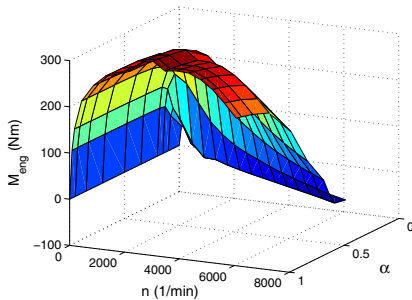


Fig. 3. Typical engine characteristics

The required torque of the engine is computed with the next expression as:

$$M_{eng} = \frac{F_l R_w}{k_0 k_g} \quad (18)$$

where  $R_w$  is wheel radius,  $k_0$  and  $k_g$  are the ratios of the driven axle and the transmission. The value of  $k_g$  depends on the current gear position. The conversion between  $M_{eng}$  and  $\alpha$  is performed through the engine characteristics, see e.g. Figure 3. This computation requires the measurement of the engine speed  $n$ , and the inversion of the characteristics based on  $M_{eng}$  and  $n$ .

The braking system in the paper is a conventional hydraulic construction. The dynamics of the braking hydraulics  $\tau$  is faster than the longitudinal motion, therefore the relationship between  $F_l$  and brake cylinder pressures is described by static equations. First, the longitudinal force is divided between the front and the rear axles, using the following expression, see Zomotor (1991):

$$F_r = -F_{fr} - \frac{mg l_2}{2h} + \sqrt{\frac{F_{fr}(l_1 + l_2) mg}{h} + \left(\frac{mg l_2}{2h}\right)^2} \quad (19)$$

where  $F_r$  and  $F_{fr}$  are the wheel forces at the rear and at the front, respectively.  $h$  represents center of gravity height,  $l_1, l_2$  are the distances between the axles and the center of gravity.  $F_{fr}$  and  $F_r$  are divided equally between the left and the right sides. Second, the wheel longitudinal forces are converted into the cylinder braking pressures, such as

$$p_i = \frac{F_i R_w}{C_{pM,i}} \quad (20)$$

where  $F_i$  is the longitudinal force of the wheel, and  $C_{pM,i}$  is the constant, which depends on the wheel brake construction.

The decision between the actuation of the driveline and braking depends on the control force  $F_l$ . If  $F_l > 0$  then throttle is activated, otherwise the braking pressures of the cylinders are increased.

## 4. SIMULATION EXAMPLES

In this section, the results of the proposed control method are presented through simulation scenarios. For simulation purposes, the CarSim vehicle dynamics software is applied. In the simulation, the data of the test vehicle are used. In the two proposed simulations, the nominal mass is set at 2037kg and the maximum mass is 2637kg.

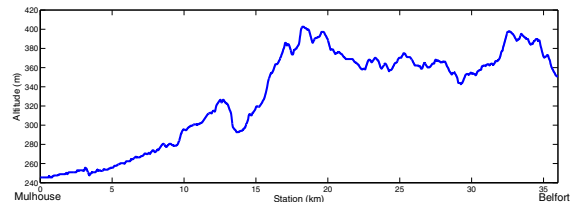


Fig. 4. Altitude of the road

The simulations based on the real topographical data of the French highway section A36 between Mulhouse and Belfort are performed, see Figure 4. The altitude and road geometry coordinates are derived from Google Earth. The proposed road is a 36km-long highway section with several

road slope changes. In the simulations the efficiency of the control system is presented, such as precise velocity tracking and robustness against mass variation and road slope change.

Two simulations are presented in the following. First, the simulation is performed using the nominal mass vehicle, while in the second simulation the results of the controlled overloaded-mass vehicle are analyzed. Figure 5(a) illustrates the velocity tracking of the nominal mass vehicle. In the simulation the road section contains several velocity regulations, which must be guaranteed. The result shows that the controlled system is able to guarantee a precise tracking. The changes in the road slope are attenuated by the robust control, while the variation of the reference signal is tracked. Figure 5(b) illustrates the control input and its components  $u_0$  for feedback control and  $u_1$  for feedforward control. The feedforward control  $u_1$  is responsible for the rejection of road slope disturbance, therefore the influence of the powerful road grade variation on the velocity tracking is reduced.

The physically applied engine throttle is illustrated in Figure 5(c). The required throttle is calculated through the torque map of the engine and the current gear ratio, see Figure 5(d). The effect of the reference velocity change is represented on the throttle actuation: at  $12km$ ,  $21km$  and  $34km$  section points the reference velocity significantly changes. Thus, the throttle is increased to guarantee the precise tracking, see Figure 5(d). The effects of the reference velocity changes in the control input signal are also represented in Figure 5(b). The handling of the reference velocity change is guaranteed by the feedback control input  $u_0$ . The generated engine torque can be seen in Figure 5(e). The brake cylinder pressures on the wheels are presented in Figure 5(f). The actuated brake pressure is calculated through the characteristics of the braking system.

Figure 6 presents the simulation examples of the full-mass vehicle ( $2637kg$ ) on the same route. The velocity tracking of the vehicle is shown in Figure 6(a). It is shown that the velocity tracking is accurate as in just as the nominal mass vehicle. Thus, the control system operates appropriately together with the mass variation. Figure 6(b) shows the control force of the full-mass vehicle. The required control input  $u_1$  is higher than in Figure 5(b), because mass variation  $m_v$  must be compensated for through an increased control input.

The increased vehicle mass requires an increased control input  $u$ , which results a more powerful engine throttle actuation, see Figure 6(c). The increases in the engine torque and brake pressures are illustrated in Figure 6(d),(e).

Finally, the designed  $\mathcal{H}_\infty$ -based cruise control guarantees the appropriate velocity tracking. Moreover, the robustness against the mass variation and the change of the road slope are analyzed and shown through the simulation examples. The proposed control algorithm yielded adequate simulation results, thus it is recommended to use it in the further implementation steps.

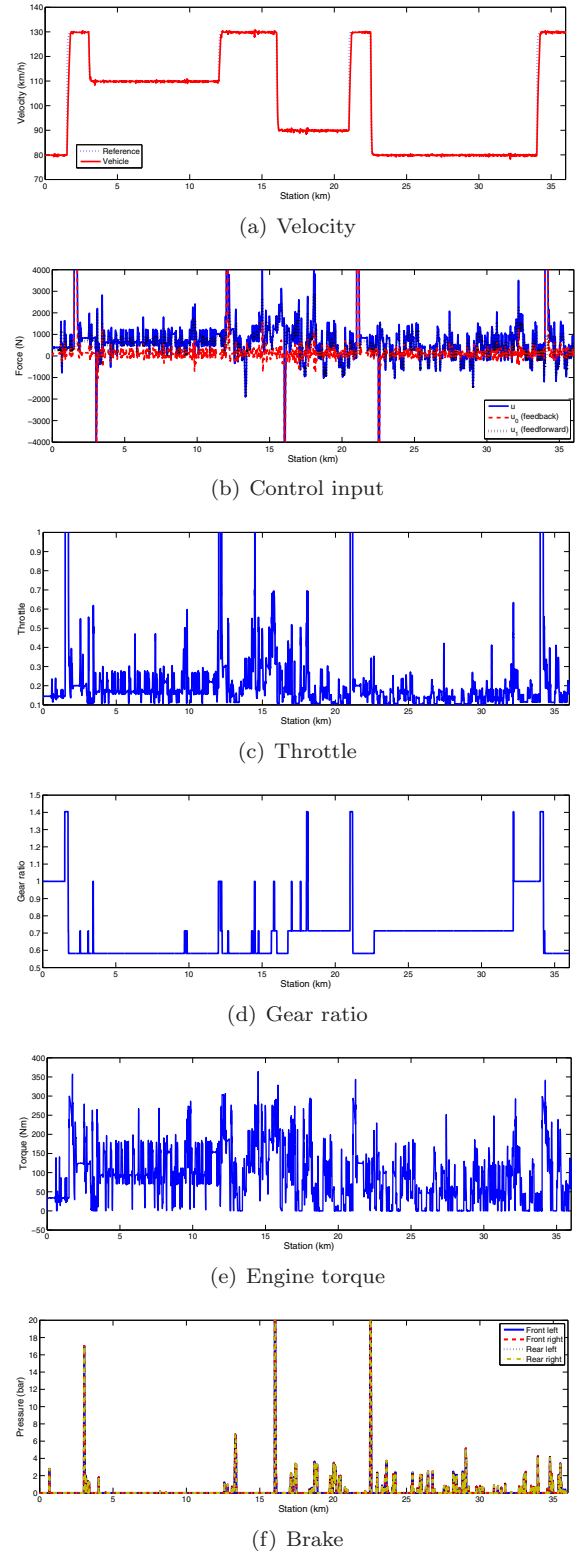


Fig. 5. Results of the first simulation

## 5. CONCLUSIONS

In the paper a control design of a cruise control system for a test vehicle is designed. The resulting control algorithm guarantees the robustness of velocity tracking against road slopes, road resistances and mass variations. The accuracy of velocity tracking is improved with the combination of a

robust optimal  $\mathcal{H}_\infty$  feedback combined with a feedforward controller. The proposed control design requires a low number of vehicle parameters, thus the method can be applied to various vehicles. The efficiency of the control is shown during simulation examples. In a near future, the proposed control algorithm will be tested on a real vehicle.

## REFERENCES

- Attia, R., Orjuela, R., and Basset, M. (2014). Nonlinear cascade strategy for longitudinal control in automated vehicle guidance. *Control Engineering Practice*, 29, 225–234.
- Borrelli, F., Bemporad, A., Fodor, M., and Hrovat, D. (2001). *Hybrid Systems: Computation and Control*, volume 2034, chapter A Hybrid System Approach to Traction Control, 162–174. Springer Berlin Heidelberg.
- Boyd, S., Ghaoui, L.E., Feron, E., and Balakrishnan, V. (1997). *Linear Matrix Inequalities in System and Control Theory*. Society for Industrial and Applied Mathematics, Philadelphia.
- Junaid, K., Shuning, W., Usman, K., and Wencheng, T. (2005). Intelligent longitudinal cruise control by quadratic minimization and robust synthesis. In *IEEE International Conference on Vehicular Electronics and Safety*, 182 – 187. Xi’an, China.
- Katriniok, A., Maschuw, J., Christen, F., Eckstein, L., and Abel, D. (2013). Optimal vehicle dynamics control for combined longitudinal and lateral autonomous vehicle guidance. In *IEEE European Control Conference*, 974 – 979. Zurich, Switzerland.
- Kolmanovsky, I. and Filev, D. (2010). Terrain and traffic optimized vehicle speed control. In *IFAC Advances in Automotive Control Conference*, 378–383. Munich, Germany.
- Lefebvre, D., Chevrel, P., and Richard, S. (2003). An H-infinity-based control design methodology dedicated to the active control of vehicle longitudinal oscillations. *IEEE Transactions on Control Systems Technology*, 11(6), 948 – 956.
- Li, S., Li, K., Rajamani, R., and Wang, J. (2011). Model predictive multi-objective vehicular adaptive cruise control. *IEEE Transactions on Control Systems Technology*, 19(3), 556 – 566.
- Lu, X. and Hedrick, J. (2005). Heavy-duty vehicle modelling and longitudinal control. *Vehicle System Dynamics*, 43(9), 653–669.
- Menhour, L., d’Andréa Novel, B., Fleiss, M., and Mounier, H. (2013). Multivariable decoupled longitudinal and lateral vehicle control: A model-free design. In *IEEE 52nd Annual Conference on Decision and Control*, 2834 – 2839. Firenze, Italy.
- Scherer, C. and Weiland, S. (2000). *Lecture Notes DISC Course on Linear Matrix Inequalities in Control*. Delft University of Technology, Delft, Netherlands.
- Vahidi, A., Stefanopoulou, A., and Peng, H. (2005). Recursive least squares with forgetting for online estimation of vehicle mass and road grade: theory and experiments. *Vehicle System Dynamics*, 43(1), 31–55.
- Xu, Z. and Ioannu, P. (1994). Adaptive throttle control for speed tracking. *Vehicle System Dynamics*, 23(1), 293–306.
- Zomotor, A. (1991). *Fahrwerktechnik, Fahrverhalten*. Vogel Verlag Und Druck.

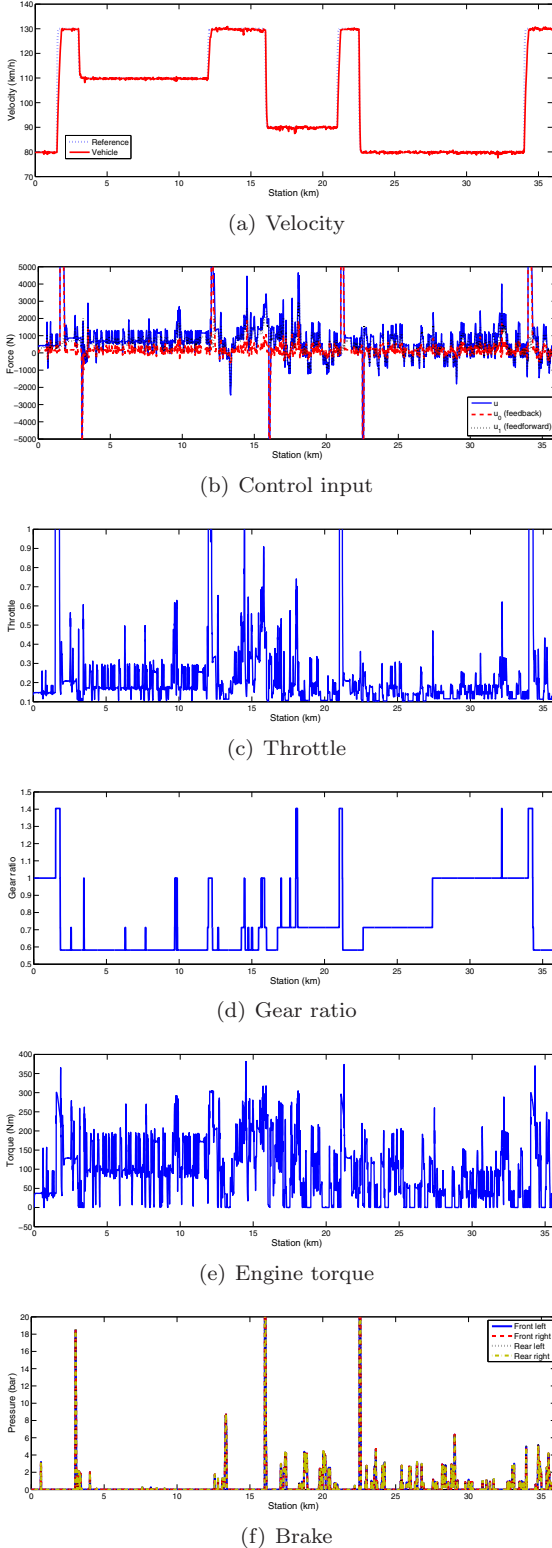


Fig. 6. Results of the second simulation